DOI:10.1021/jf902381e

JOURNAL OF AGRICULTURAL AND FOOD CHEMISTRY
ARTICLE

Kinetics of Anthocyanin Degradation and Browning in Reconstituted Blackberry Juice Treated at High Temperatures (100−180 °C)

Nadiarid Jiménez,[†] Philippe Bohuon,*[,‡] Janice Lima,[§] Manuel Dornier,[‡] Fabrice Vaillant,[∥] and Ana Mercedes Pérez[⊥]

[†]Escuela de Tecnología de Alimentos, Universidad de Costa Rica, Apartado Postal 11501-2060, San José, Costa Rica, [‡]Montpellier SupAgro, UMR QualiSud, 1101 avenue Agropolis, CS 24501, 34093 Montpellier Cedex 5, France, [§]Embrapa Agroindústria Tropical, Rua Dra Sara Mesquita, 2270 - Planalto do Pici, CEP 60511-110, Fortaleza, Ceará, Brazil, [∥]CIRAD, UMR QualiSud, 40/15, 73 rue Jean François Breton, 34398 Montpellier Cedex 5, France, and [⊥]Centro Nacional de Ciencia y Tecnología de Alimentos (CITA), Universidad de Costa Rica, Apartado Postal 11501-2060, San José, Costa Rica

Monomeric anthocyanin degradation and nonenzymatic browning (NEB) index have been determined in reconstituted blackberry juice heated at high temperature in a hermetically sealed cell. Statistical analysis demonstrated that, when the temperature range (100−180 °C) was divided into two subranges (100−140 and 140−180 °C) for anthocyanin degradation, reaction kinetics were well represented by two sequential first-order reactions. The activation energy for NEB from 100 to 180 °C (106 kJ·mol^{-1}) was slightly higher than the anthocyanin value at the lower temperature range (92 kJ·mol^{-1}), but was more than twice the value for the higher range (44 kJ·mol^{-1}). The reaction rate constant at 140 °C for anthocyanin degradation (3.5×10^{-3} s^{-1}) was two times that for the NEB index (1.6×10^{-3} s^{-1}). Hence, anthocyanin degradation was faster than the appearance of NEB products. The non-isothermal method developed allows estimating kinetic parameters and thereby generating temperature profiles of heat processes that would help preserve the nutritional properties of foods during high-temperature processes.

KEYWORDS: Blackberry juice; kinetics modeling; anthocyanins; nonenzymatic browning; heat treatment

INTRODUCTION

Blackberries are particularly interesting because of their high contents of phenolic compounds, especially of ellagitannins and anthocyanins (*1*, *2*). These compounds possess a significant antioxidant capacity (free-radical scavenging and metal chelating). Hence, they play a potentially beneficial role in human health by reducing risks of cancer, cardiovascular disease, and other pathologies (*3*, *4*).

Anthocyanins are polyphenolic pigments, responsible for the red, blue, and purple colors of many fruits and vegetables. However, they readily degrade during food processing and storage, being highly reactive to factors such as oxygen, light, pH, and temperature. The last two in particular may dramatically affect color quality and the nutritional properties of products (*5*).

Food processing usually involves the use of heat treatments to effectively preserve foodstuffs and provide desirable sensory properties. However, nutritional quality is often compromised. If optimal color, and nutritional and functional qualities are to be maintained, anthocyanin degradation must be minimized during processing (*6*).

*Author to whom correspondence should be addressed. Tel: +33 4 67 615726. Fax: +33 4 67 615728. E-mail: philippe.bohuon@supagro.inra.fr.

Several authors have studied the heat degradation of anthocyanins (*7*−*16*) and have reported on kinetic parameters (activation energy and reaction rate constant) for a wide variety of anthocyanin-rich products (**Table 1**). The parameters were obtained through first-order kinetics and modeling temperature dependence according to the Arrhenius equation. Most of the studies were conducted at temperatures below 100 °C, which may be considered as isothermal treatments.

However, some heat processes for anthocyanin-rich foodstuffs involve temperatures of more than 100 °C, for example, vacuum-frying blue potatoes (*17*), sterilizing grape pomace (*10*), extruding corn meal with blueberry and grape anthocyanins for breakfast cereals (*18*), and spray-drying açaí pulp (*19*). Few kinetic data obtained at higher temperatures have also been published (*9*, *10*). Nonetheless, at temperatures of more than 100 °C, heat treatments are non-isothermal, as the heating and cooling stages are too long to be ignored. Non-isothermal methods must therefore be used to estimate the kinetic parameters at these high temperatures (*9*).

Such methods evaluate the cumulative effect of time−temperature history ($T^{(t)}$) on anthocyanin degradation ($C^{(t)}$) and nonenzymatic browning ($B^{(t)}$) through the determination of kinetic parameters (E_a and k_{ref}). These parameters are obtained by

 Published on Web 01/28/2010

Table 1. Published Data for Kinetic Parameters (Activation Energy E_a and Rate Constant k) of Anthocyanin Thermal Degradation of Some Products

ref	product	temp range (°C)	anthocyanin determination	E_a (kJ·mol^{-1})	k ($\times 10^{-6}$s^{-1})
7	blood orange juice	30−90	pH differential	66.0	14.6−166.0
	blackberry juice			37.0	8.1−74.8
	roselle extract			51.1	2.9−75.1
8	blood orange	70−90			
	cyanidin 3-glucoside		pH differential	75.4	14.8−63.3
			RP-HPLC	74.6	15.3−64.6
	cyanidin 3-(6″-malonyl) glucoside		pH differential	79.5	10.3−47.8
			RP-HPLC	75.8	16.4−70.7
9	blackcurrant juice	4−140	pH differential	81 ± 3	0.04−2765
10	grape pomace	126.7	HPLC	65 ± 33	2382 ± 100
11	purple corn cob (pH 4)	70−90	pH differential	18.3	16.6−25.7
12	blackberry juice (8.9 °Brix)	60−90	pH differential	58.9	11.5−65.7
13	purple-flesh potatoes	25−98	color retention	72.5	0.19−90.5
	red-flesh potatoes			66.7	0.08−20.1
	grape			75.0	0.17−79.2
	purple carrot			81.3	0.03−27.9
14	black carrot (pH 2.5)	70−90	pH differential	78.1	7.7−34.5
15	sour cherry juice (15 °Brix)	50−80	pH differential	68.5	1.1−9.4
16	blackberry juice (BJ)	24−70	pH differential	61.8	0.7−196.4
	BJ + HMF[a]			54.6	1.2−232.5
	BJ + furfural			52.9	1.3−246.4

[a]HMF: 5-Hydroxymethylfurfural.

minimizing the sum of squares error (SSE) between experimental and predicted data. As the model is nonlinear for parameters, no explicit analytical solutions are available for the confidence intervals. Hence, the confidence interval for each parameter must be determined by methods such as Monte Carlo simulations (*20*).

This study aimed, first, to experimentally quantify in reconstituted blackberry juice the total monomeric anthocyanin content ($C^{(t)}$), total polyphenol content, antioxidant capacity (ORAC), and nonenzymatic browning index ($B^{(t)}$) during heat treatments; second, to develop a kinetic model to describe $C^{(t)}$ and $B^{(t)}$ in heat situations, using a non-isothermal method; and third, to discuss the advantages of using high-temperature short-time (HTST) treatments for blackberries to reduce the impact of heat on product quality during different food processes.

MATERIALS AND METHODS

Blackberry Juice. Fully ripe tropical highland blackberries (*Rubus adenotrichus*) were harvested in Cartago region, Costa Rica (1500 m above sea level) and frozen at −10 °C. The frozen blackberries were then thawed at 5 °C for 12 h and pressed with a discontinuous hydraulic press (OTC-25-ton H-frame Hydraulic Shop Press, series Y125, Owatonna, MN) to obtain the juice. The juice was then freeze-dried and vacuum-packed in laminated metallic bags, and kept frozen at −18 °C.

Preparing Reconstituted Blackberry Juice. Lyophilized blackberry juice was reconstituted by dilution at 10 g·100 mL^{-1} with distilled water and mixed at 1800 rpm for 30 min in a vibrating shaker (Heidolph MULTI REAX, Schwabach, Germany). The juice was degasified before heat treatment by bubbling argon for 30 min until the dissolved oxygen concentration was less than 1 mg·L^{-1}, as determined by a MultiLine P3 pH/Oximeter with a CellOx 325 probe (WTW, Weilheim, Germany).

Heating Device and Conditions. Reconstituted blackberry juice was pipetted into the test cell at room temperature ($T^0 = 21 \pm 3$ °C). Juice was heated in a hermetically sealed test cell (**Figure 1**) that was custom-designed in stainless steel (type 316). The inner diameter was 50 mm and the inner height 7 mm. Reactor capacity was 1×10^{-2} L of samples. To improve heating uniformity, the test cell was divided into eight compartments by plate-fin spokes that were 1 mm thick to increase heat exchange. Sample temperatures within the closed reactor were recorded every five seconds with a 1.5 mm thick Type J thermocouple with a stainless steel sheath (model 405-163, TC Direct, Dardilly, France) located at the geometrical center of one compartment and connected to a data logger (ALMEMO 2290-8 V5, Ahlborn, Holzkirchen, Germany), using AMR Data-Control V5.13 Software (Ahlborn, Holzkirchen, Germany).

The test-cell thermocouple was calibrated in an oil bath against a precalibrated thermometer and all temperature measurements corrected. A Viton O-ring (∅ = 56.82 × 2.62 mm) ensured the test cell's hermetic sealing, preventing mass transfer of water and oil, which could interfere in component degradation.

Heat treatment was performed in two consecutive oil baths with thermostats. The first bath, a four liter oil bath (MR Hei-End, Magnetic Hot plate Stirrer, Heidolph Instruments, Schwabach, Germany), was maintained at a high temperature (T_∞ = 195 °C) to quickly increase juice temperature. The bulk temperature (T_∞) was achieved due to silicon oil (Thermofluid P20.275.50, Huber Kältemaschinenbau, Offenburg, Germany) and controlled with a Pt 100 temperature sensor (Heidolph Instruments, Schwabach, Germany). The second bath, a five liter deep-fat fryer (model KPB 50, Kenwood, Villepinte, France), was heated to trial temperatures (T_∞ = 100−180 °C). The time interval between the first and second thermostat oil baths did not exceed 3 s. In each bath, the bulk of the oil volume was stirred at 1200 rpm with a EUROSTAR electronic overhead stirrer (IKA-Werke, Staufen, Germany). The radial flow of the stirring unit produced turbulence and ensured homogenization of the temperature field. When the reactor was first plunged into the oil, the maximum local temperature variation was 5 °C below T_∞. The test cell was held and maintained submerged with a wire.

For the kinetic experiments, samples were taken at different heating times, which were chosen according to treatment temperatures. After each heat treatment, the test cell was immediately cooled in an ice−water bath and dried with paper towel. The sample was then removed from the cell and stored at 4 °C overnight until analysis.

After heat treatment, the juice was centrifuged at 12074*g* for 10 min, using a Sigma 1-15 Microfuge (Fisher Bioblock Scientific, Illkirch, France). It was then filtered with a Minisart SRP 25 filter (0.45 μm pore size; Sartorius AG, Göttingen, Germany) to separate suspended solids formed during heating and cooling.

Analytical Methods. *Physicochemical Analysis*. Reconstituted blackberry juice was analyzed for pH, titratable acidity (citric acid at g·L^{-1}), and total soluble solids (g·kg^{-1}), using standard methods (*21*). All analyses were done in quintuplicate and results reported with 95% confidence intervals (standard deviation × 2.57, where n = 5).

Total Monomeric Anthocyanin Content. Total monomeric anthocyanin content (C) was determined by the pH differential method (*22*, *23*). Juice absorbance was measured at pH 1.0 and 4.5 at wavelengths of maximum absorbance (510 nm) and at 700 nm to correct for haze. Measurements were performed with a microplate spectrofluorimeter (Infinite 200, Tecan France S.A.S., Lyon, France), using 96-well polypropylene plates. Total monomeric anthocyanins were expressed as cyanidin 3-glucoside

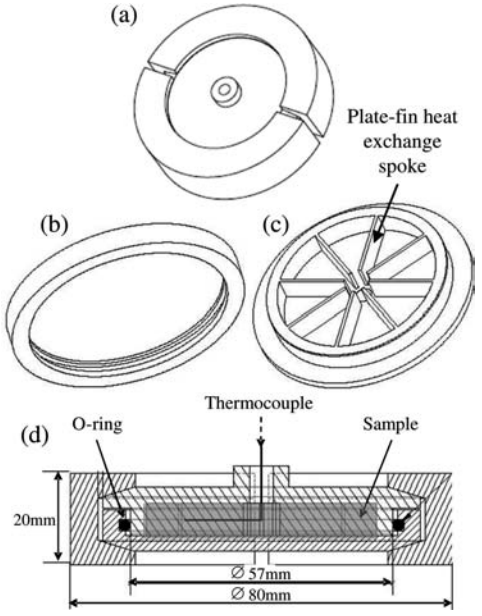

Figure 1. Schematic diagram of test cell. (**a**) General assembly, (**b**) cell cap, (**c**) cell cupel, (**d**) lateral view of cell assembly.

equivalents, the most prevalent anthocyanin in *R. adenotrichus* at 95% (*2*):

$$C\ (\mathrm{mg \cdot L^{-1}}) = \frac{A \times \mathrm{MW} \times \mathrm{DF}}{\varepsilon \times l} \times 10^3 \qquad (1)$$

where A or absorbance $= (A_{510\mathrm{nm}} - A_{700\mathrm{nm}})(\mathrm{pH}_{1.0}) - (A_{510\mathrm{nm}} - A_{700\mathrm{nm}})(\mathrm{pH}_{4.5})$; MW or molecular weight $= 449.2\ \mathrm{g \cdot mol^{-1}}$ for cyanidin 3-glucoside; DF or dilution factor $= 10$ to 50; ε or molar extinction coefficient $= 26\,900\ \mathrm{L \cdot mol^{-1} \cdot cm^{-1}}$; l or path length $= 0.52$ cm (calculated for the specific well geometry with 200 μL of solution) and 10^3 = conversion factor from g to mg.

The pH differential method was validated by comparing selected results with the HPLC method (*2*), obtaining coefficients of variation between 3 and 7% (results not shown).

Total Polyphenol Content. The total polyphenol content (TP) was determined by the Folin−Ciocalteu assay as modified according to Georgé et al. (*24*), and expressed as gallic acid equivalents in $\mathrm{mg \cdot L^{-1}}$.

Antioxidant Capacity. An oxygen radical absorbance capacity (ORAC) assay was performed in accordance with Ou et al. (*25*), using a microplate spectrofluorimeter with 96-well plates made in black polypropylene (*26*). The ORAC value was expressed as Trolox equivalents ($\mu\mathrm{mol \cdot L^{-1}}$).

Nonenzymatic Browning Index. Nonenzymatic browning index (B) was calculated according to Buglione and Lozano (*27*) for red juices. A microplate spectrofluorimeter was used, with 96-well plates made in transparent polypropylene. The absorbance of reconstituted blackberry juice was measured at pH 1.0 at two wavelengths: 510 nm for anthocyanin maximum absorbance, and 420 nm for absorbance of both browning products and anthocyanins. The nonenzymatic browning index was calculated as follows:

$$B = A_{510}/A_{420} \qquad (2)$$

The nonenzymatic browning equilibrium value (B^{∞}) was determined after prolonged heating at high temperature. Reconstituted blackberry juice was heated at 180 °C for 30 and 45 min in triplicate. The B index was then calculated. No significant difference ($p < 0.05$) was found between B values for the two heating times, showing that the equilibrium value was reached at $B^{\infty} = 0.25 \pm 0.02$.

Repeatability of the Heat Treatment and Subsequent Physicochemical Analyses. To assess the standard error of the heat treatments and subsequent analyses for the different responses, three replicates of the experiment were performed at 140 °C for 1, 2, 4, 6, and 8 min. The resulting standard error was found to be 5% for monomeric anthocyanin content and 3% for the nonenzymatic browning index. For the other temperatures

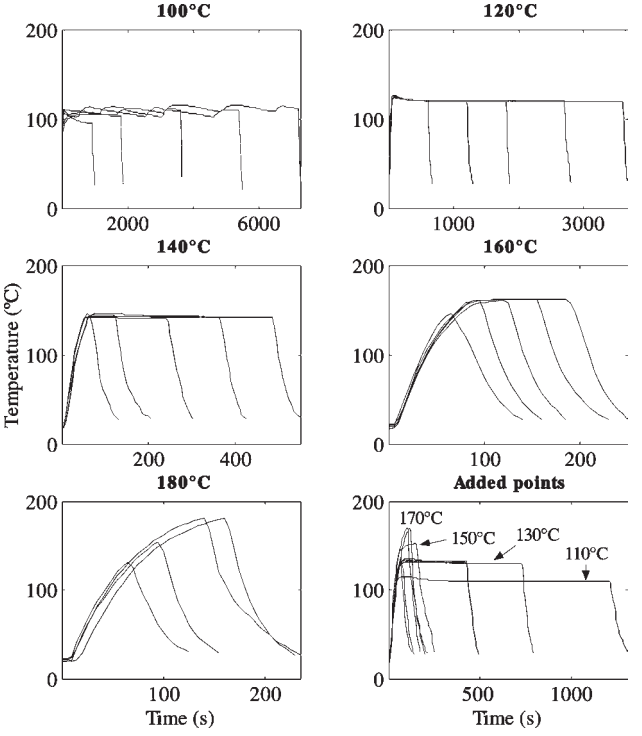

Figure 2. Time−temperature profiles ($T^{(t)}$) for reconstituted blackberry juice samples heated from 100 to 180 °C in a hermetically sealed cell.

(100, 120, 160, and 180 °C), only one experiment was performed for each time.

Kinetic Model Development. Kinetic modeling was conducted to develop a useful tool, which, in association with a heat transfer model, could predict anthocyanin degradation and nonenzymatic browning in reconstituted blackberry juice exposed to different heat processes (deep-fat frying, spray drying, sterilization, extrusion, and others) under isothermal or non-isothermal conditions (heating, maintaining, and cooling). Equations are therefore presented to evaluate the cumulative effects of any time−temperature history ($T^{(t)}$) on anthocyanin degradation ($C^{(t)}$) and nonenzymatic browning ($B^{(t)}$).

Selecting Models. Two cases were considered for the description of the anthocyanins content ($C^{(t)}$) and nonenzymatic browning index ($B^{(t)}$) behavior during heat treatment.

Case 1: $C^{(t)}$ and $B^{(t)}$ reactions were described in terms of one irreversible first-order kinetic.

$$\frac{\mathrm{d}X^{(t)}}{\mathrm{d}t} = -k_X X^{(t)} \qquad (3)$$

where $X^{(t)}$ could be $C^{(t)}$ or $(B^{(t)} - B^{\infty})$; k_X represents the rate constants. B^{∞} was determined experimentally as $B^{\infty} = 0.25 \pm 0.02$.

Case 2: $C^{(t)}$ and $B^{(t)}$ reactions were described in terms of two sequential irreversible first-order kinetics.

$$\frac{\mathrm{d}X^{(t)}}{\mathrm{d}t} = -(k_{X1} + k_{X2})X^{(t)} \text{ with } \begin{cases} k_{X1} = 0 \text{ at } T^{(t)} > T_{\mathrm{transition}} \\ k_{X2} = 0 \text{ at } T^{(t)} \leq T_{\mathrm{transition}} \end{cases} \qquad (4)$$

where $X^{(t)}$ could be $C^{(t)}$ or $(B^{(t)} - B^{\infty})$; k_{X1} and k_{X2} are the rate constants at the first and second temperature ranges.

The rate constant k_X or k_{Xi} ($\mathrm{s^{-1}}$) varied with the system's absolute temperature, T (K), according to the Arrhenius law, as follows:

$$k_{Xi} = k_{Xi\mathrm{ref}} \exp\left[\frac{-E_{\mathrm{a}Xi}}{R}\left(\frac{1}{T^{(t)}} - \frac{1}{T_{\mathrm{ref}i}}\right)\right] \qquad (5)$$

where $k_{Xi\mathrm{ref}}$, $E_{\mathrm{a}Xi}$, and R were, respectively, the rate constant at the reference temperature ($\mathrm{s^{-1}}$), the apparent activation energy ($\mathrm{J \cdot mol^{-1}}$) for the rate constant during the i temperature range, and the gas constant

($8.314\ J \cdot mol^{-1} \cdot K^{-1}$). The reference temperature was chosen from the middle of the i studied temperature range, expressed as follows:

$$T_{refi} = \frac{1}{n}\sum_{i=1}^{n} T_i \quad (6)$$

During heat treatment, non-isothermal stages (heating, maintaining, and cooling) were recorded. Each time−temperature profile ($T^{(t)}$; **Figure 2**) was fitted with a cubic smoothing spline (MATLAB, version 6.5, The MathWorks Inc., Natick, MA).

Parameter Estimation and Statistical Methods. The non-isothermal degradation of compound X during heat treatment was taken into account in eqs **3** or **4** with **5**. Hence, the X value, predicted at time t ($\hat{X}^{(t)}$), was calculated by time integration (general case 2), as follows:

$$\hat{X}^{(t)}/X^0 = \exp(-k_{X1ref}\beta_{X1} - k_{X2ref}\beta_{X2}) \text{ with } \begin{cases} k_{X1ref} = 0 \text{ at } T^{(t)} > T_{transition} \\ k_{X2ref} = 0 \text{ at } T^{(t)} \le T_{transition} \end{cases} \quad (7)$$

where $\hat{X}^{(t)} = \hat{C}^{(t)}$, or $\hat{X}^{(t)} = (\hat{B}^{(t)} - B^{\infty})$, for anthocyanin content kinetic or nonenzymatic browning index kinetic, respectively. β_{Xi} is the time−temperature history for X during the i temperature range, and corresponds to the equivalent isothermal time at the reference temperature (T_{refi}).

$$\beta_{Xi} = \int_0^t \exp\left[\frac{-E_{aXi}}{R}\left(\frac{1}{T^{(t)}} - \frac{1}{T_{refi}}\right)\right] dt \quad (8)$$

The integral of eq **8** was calculated as the direct analytical integral of the cubic smoothing spline function of $\exp[-E_{aXi}(1/T^{(t)} - 1/T_{refi})/R]$ with a regularization parameter of 0.99 (MATLAB, version 6.5, The MathWorks Inc., Natick, MA). There were two parameters (k_{Xiref} and E_{aXi}) to be estimated from the collected data.

As the model was nonlinear for parameters, the parameters cannot be solved directly, but must be solved by nonlinear regression. The parameters were iteratively adjusted to the goodness-of-fit merit function, using the minimization procedure of the Nelder−Mead simplex method (*28*) with the MATLAB software (MATLAB, version 6.5, The MathWorks Inc., Natick, MA). This merit function was the mean of squares error (MSE) between experimental ($X^{(t)}$) and predicted ($\hat{X}^{(t)}$) data:

$$MSE = \frac{1}{(n-p)}\sum_{i=1}^{n} (\hat{X}^{(t_i)} - X^{(t_i)})^2 \quad (9)$$

where n is the number of data and p the number of parameters (here, $p = 2$).

The minimum of the merit function was searched with different initial values for the parameters to avoid obtaining a local minimum (*29*). Because the model was nonlinear for parameters, no explicit analytical solutions could be obtained for the confidence intervals, resulting only in approximate values (*29*). Consequently, the confidence interval for each parameter was determined via Monte Carlo method (*20*). There were four steps involved in our method.

Step 1: The generation of a large number of simulated data sets from the experimental values. Simulated data ($\tilde{X}^{(t)}$) was generated by superposition

Table 2. Main Characteristics of Reconstituted Blackberry Juice (*Rubus adenotrichus*) Used for Kinetic Experiments (Mean Values ± 95% Confidence Interval with $n = 5$)

pH	2.8 ± 0.1
total soluble solids ($g \cdot kg^{-1}$)	88 ± 3
titrable acidity (g of citric acid $\cdot L^{-1}$)	25 ± 1
anthocyanins (mg of cyanidin 3-glucoside $\cdot L^{-1}$), C^0	554 ± 13
total polyphenols (mg of gallic acid $\cdot L^{-1}$)	2936 ± 90
ORAC (μmol of Trolox $\cdot$ (g of DM)$^{-1}$)	306 ± 22
nonenzymatic browning index (A_{510}/A_{420}), B^0	2.43 ± 0.08

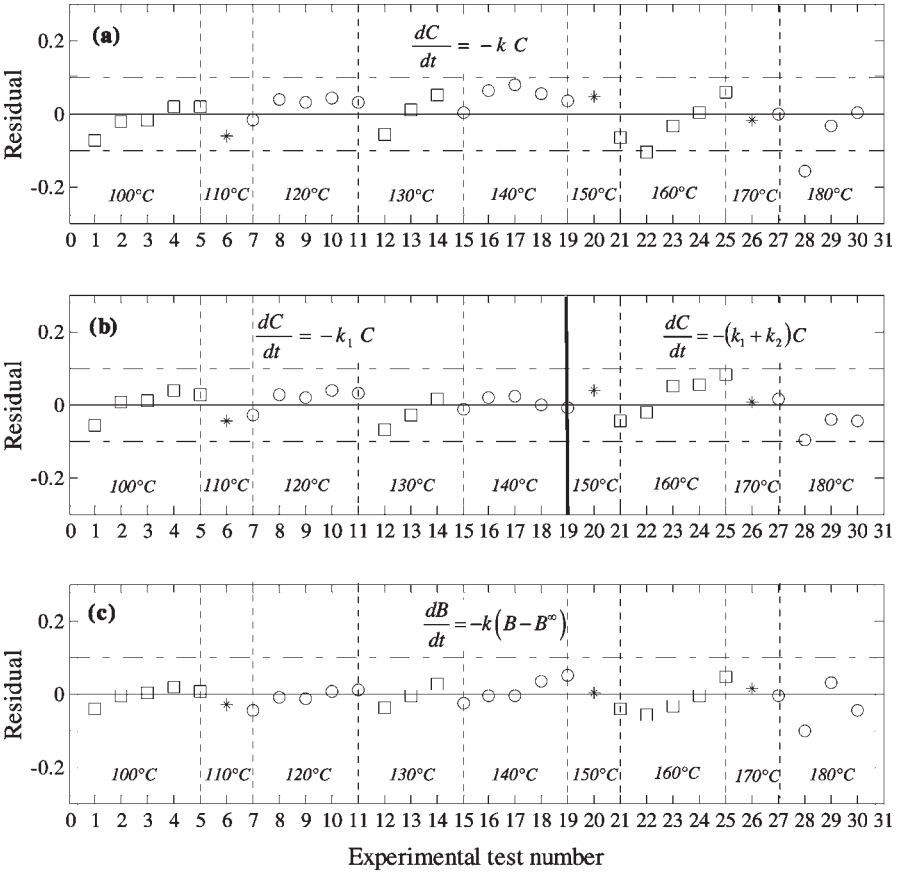

Figure 3. Residual plot of anthocyanin content ($C^{(t)}$) and nonenzymatic browning ($B^{(t)}$) at different temperatures for the single (**a**, **c**) and sequential (**b**) first-order kinetics.

Table 3. Estimated Kinetic Parameters ($\bar{E}_a$ and $\bar{k}_{ref}$) of Anthocyanin Thermal Degradation and Nonenzymatic Browning[a]

			optimized parameters			
reaction	temp range (°C)	T_{ref} (°C)	$\bar{E}_a$ (kJ·mol^{-1})	$\bar{k}_{ref}$ ($\times 10^{-3}$ s^{-1})	$k_{140\ °C}$[b] ($\times 10^{-3}$ s^{-1})	RMSE[c]
anthocyanins ($C^{(t)}/C^0$)	[100−140]	120	92 ± 8	0.90 ± 0.08	3.5 ± 0.5	0.06
	[140−180]	160	44 ± 40	20 ± 3	11 ± 7	0.12
nonenzymatic browning ($B^{(t)} - B^\infty$)/($B^0 - B^\infty$)	[100−180]	140	107 ± 3	1.62 ± 0.07	1.62 ± 0.07	0.04

[a] Mean values ± 95% confidence interval determined with Monte Carlo simulations: 2,000 sets of $C^{(t)}$ and $B^{(t)}$ data randomly with 5% and 3% of uncertainty. [b] Reaction rate constant at 140 °C. [c] RMSE: root mean square error between experimental and predicted $C^{(t)}$ and $B^{(t)}$ data.

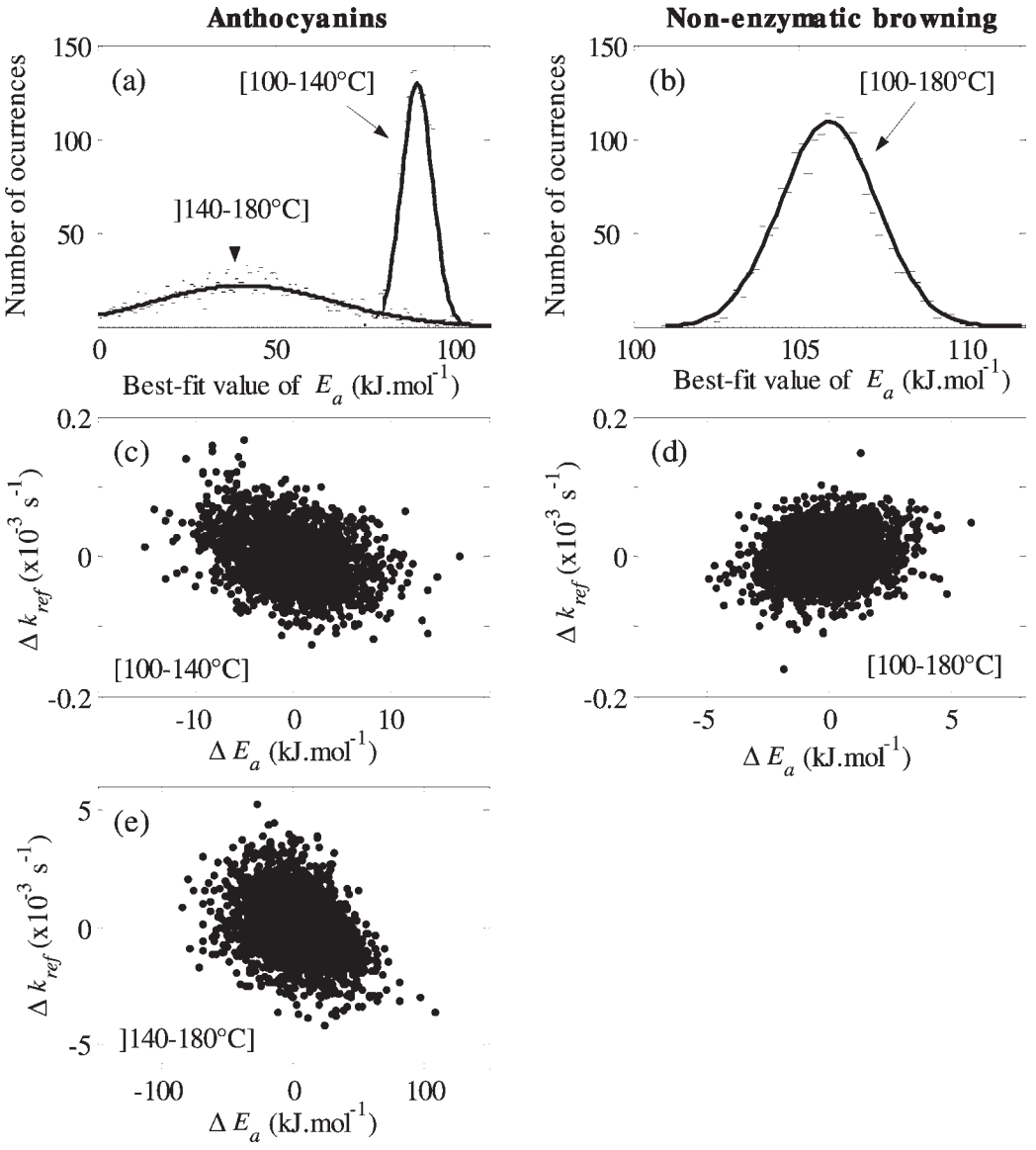

Figure 4. Monte Carlo simulations to estimate the uncertainties in the parameters and their correlation for anthocyanin degradation and nonenzymatic browning index. Histogram for activation energy values (solid lines are normal distributions) (**a** and **b**), and correlation between E_a and k_{ref} for different temperature ranges (**c**, **d** and **e**). Results of 2,000 simulations.

of a pseudo random noise on the experimental data ($X^{(t)}$). The noise reflected the experimental uncertainty ($u_{X(t)}$).

$$\tilde{X}^{(t)} = X^{(t)} + u_{X^{(t)}}\delta \quad (10)$$

where $\tilde{X}^{(t)}$ is the simulated data; $u_{X(t)}$ is the uncertainty of $X^{(t)}$, determined experimentally (equivalent to the standard deviation for a Gaussian distribution); δ is a random number whose elements are normally distributed, with a mean of 0 and a variance of 1. All uncertainties were amplified as follows:

$$U_{X^{(t)}} = \varphi u_{X^{(t)}} \quad (11)$$

where φ is the covering factor ($\varphi = 1.96$ for 95% confidence interval) (*30*).

Step 2: The estimation of kinetic parameters ($k_{Xi\text{ref}}$ and E_{aXi}) from each simulated data set. For a given operating condition, m sets of anthocyanin content ($C^{(t)}$) and nonenzymatic browning index ($B^{(t)}$) data were randomly drawn, using eq **10** (m = 2,000). Then, each simulated data set was fitted to determine the best-fit values of the kinetic parameters ($k_{Xi\text{ref}}$ and E_{aXi}), and m values of parameters were identified from m separate data sets. The $k_{Xi\text{ref}}$ and E_{aXi} were checked for normal distribution, using the Kolmogorov−Smirnov test.

Step 3: The representation of histograms from the tabulated kinetic parameters, to obtain discrete approximations of the model parameters confidence probability distributions. The results were therefore expressed as mean values of parameters ($\bar{k}_{Xi\text{ref}}$ and $\bar{E}_{aXi}$) associated with their

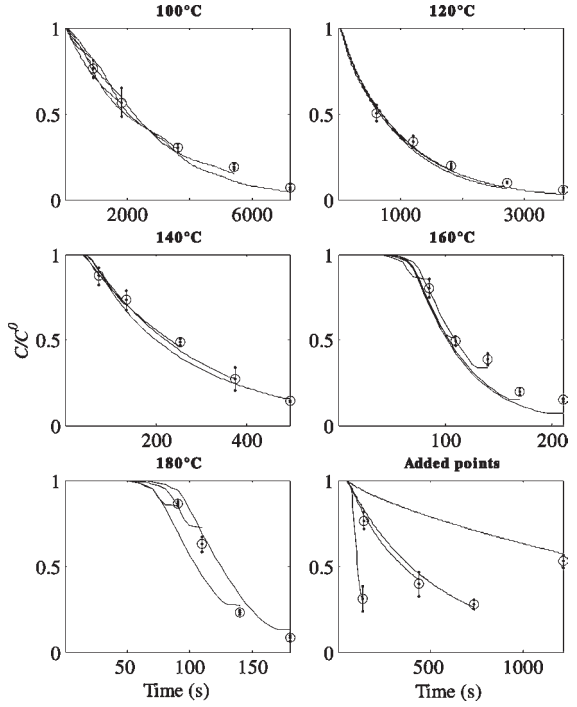

Figure 5. Degradation kinetics of monomeric anthocyanins ($C^{(t)}$) during thermal treatment from 100 to 180 °C. Experimental data (○) and predicted curves from two sequential first-order kinetics ([100−140 °C] then [140−180 °C]). Bars represent 95% confidence interval (n = 5).

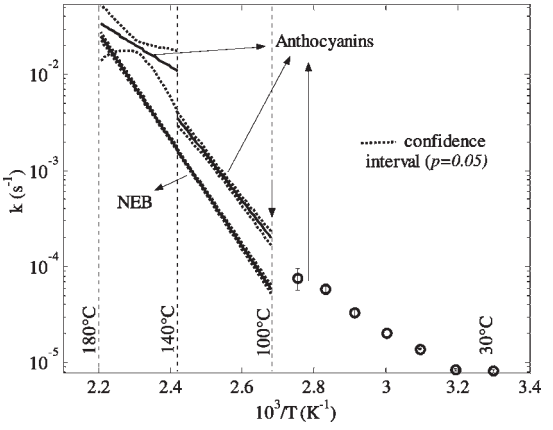

Figure 6. Arrhenius plot describing the temperature dependence of nonenzymatic browning (NEB) and anthocyanin degradation rate constant (k) of reconstituted blackberry juice (*R. adenotrichus*) from 30 to 90 °C (*7*) and 100 to 180 °C (present study).

standard deviation. All these uncertainties were amplified by factor φ = 1.96, corresponding to a 95% confidence interval for parameters. Relative amplified uncertainty, expressed as percentage, was calculated with reference to the mean value obtained after averaging the m values.

Step 4: The analysis of the correlation between the two parameters by the representation of scatter plots (Δk_{Xiref} versus ΔE_{aXi}).

RESULTS AND DISCUSSION

Initial Characteristics of Reconstituted Blackberry Juice. Table 2 presents the values of some physicochemical properties of the reconstituted blackberry juice. Results are consistent with those reported in literature for blackberry juice (*7*, *12*) and other berries belonging to the *Rubus* genus (*31*), particularly *R. adenotrichus* (*2*). That is, blackberry juice is a good source of natural antioxidants. The predominance of the anthocyanin

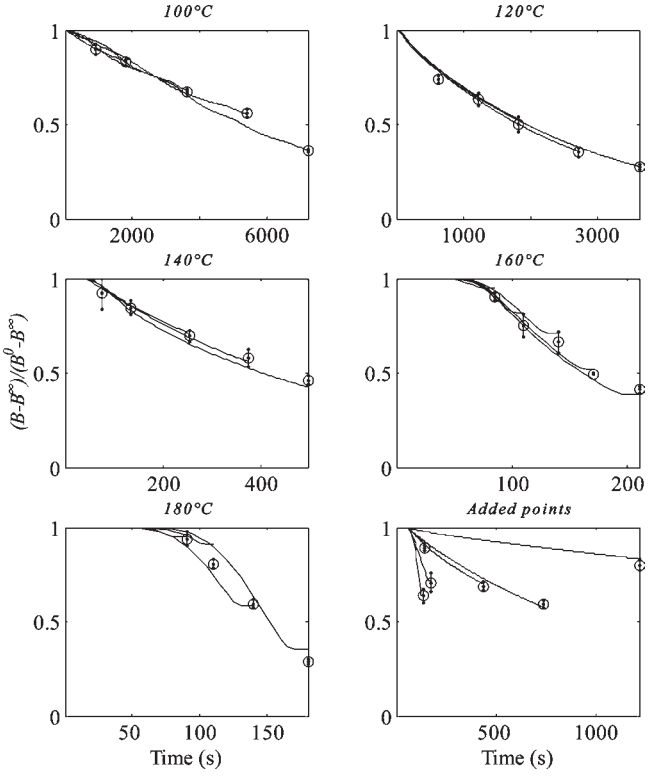

Figure 7. Kinetics of nonenzymatic browning during thermal treatment from 100 to 180 °C. Experimental data (○) and predicted curves for each trial. Bars represent 95% confidence interval (n = 5).

cyanidin 3-glucoside in blackberry juice (*R. adenotrichus*) was confirmed by comparing the juice's HPLC chromatograms with those of standard kuromanine (cyanidin 3-glucoside), results not shown.

Kinetic Parameter Estimation. Monomeric anthocyanin content ($C^{(t)}$), total polyphenol content ($TP^{(t)}$), antioxidant capacity ($ORAC^{(t)}$), and nonenzymatic browning index ($B^{(t)}$) were measured experimentally in the juice for different time−temperature treatments. The results for $TP^{(t)}$ and $ORAC^{(t)}$ are not considered in our study, as neither presented a defined pattern. They are global measurements that can be affected by the presence of water-soluble Maillard reaction products that may have antioxidant activity (*32*).

For the monomeric anthocyanin content ($C^{(t)}$) and nonenzymatic browning index ($B^{(t)}$), the non-isothermal method was used to estimate kinetic parameters.

Figure 3 shows the residual plots of anthocyanin content (single and sequential first-order kinetics) and nonenzymatic browning index. In **Figure 3a**, for the single first-order kinetic, the residues ($C^{(t_i)} - \hat{C}^{(t_i)}$) of each experimental trial were calculated from the parameters estimated for the temperature range 100 to 180 °C (E_a = 101 kJ·mol^{-1} and $k_{ref} = 4 \times 10^{-3}$ s^{-1}, for T_{ref} = 140 °C). An apparent trend was observed throughout the tests. In the initial section most of the residual content of anthocyanins was underestimated and, after 140 °C, most of the residual content was overestimated. Distribution of residues was considerably improved when a transition temperature of 140 °C for the sequential analysis was considered (**Figure 3b**). Residual values of NEB index obtained from a single first-order kinetic are shown in **Figure 3c**, and no specific pattern was observed.

Table 3 shows the optimized kinetic parameters for $C^{(t)}$ and $B^{(t)}$, considering two sequential first-order kinetics for the anthocyanin thermal degradation and one first-order kinetic for nonenzymatic browning. The confidence intervals of these kinetic

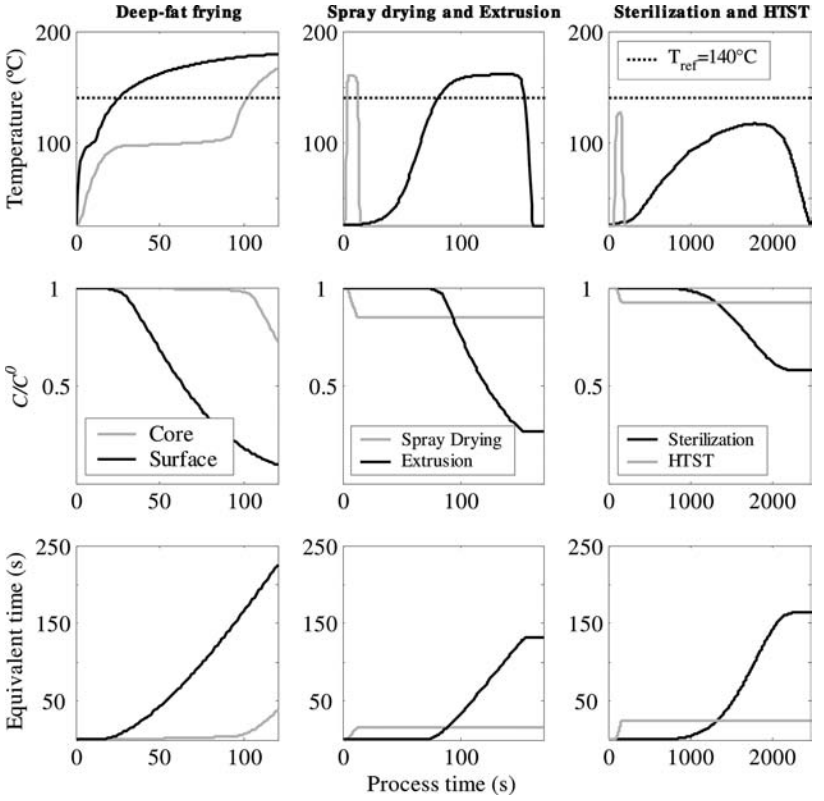

Figure 8. Simulated non-isothermal heating profiles, anthocyanin degradation curves and equivalent isothermal time (with T_{ref} =140 °C) for different applications: deep-fat frying, spray drying, extrusion, conventional and HTST sterilization.

parameters were determined via Monte Carlo simulations, using 2,000 data sets that generate the same number of best-fit values for the kinetic parameters (k_{Xref} and E_{aX}). According to van Boekel (*33*), the Monte Carlo method provides the most accurate probability distribution of the model parameters, and it also provides information on the correlation between parameters. **Figure 4** shows the results of the Monte Carlo simulations, where a normal distribution of the parameter E_a was obtained for $C^{(t)}$ and $B^{(t)}$ as shown in **Figures 4a** and **4b**. In **Figure 4a**, a large standard deviation was observed for the activation energy of anthocyanins at temperatures above 140 °C, probably due to scarce experimental data computed within this region. **Figures 4c** to **4e** reveal the lack of correlation between the kinetic parameters E_a and k_{ref} for both responses, as a result of reparametrization (*29*, *33*), through the introduction of a reference temperature.

Monomeric Anthocyanin Content. Figure 5 illustrates the good fit obtained between experimental data and the lower end of predicted curves, using the optimized kinetic parameters shown in **Table 3** for the sequential analysis discussed above ($T_{transition}$ = 140 °C). The impact of temperature on anthocyanin degradation is sufficiently significant at higher temperatures that the time scale of the graphs must be changed from 0 to 6,000 s for the 100 °C treatments, and from 0 to 200 s for higher temperatures. In fact, anthocyanin degradation at high temperatures (T > 140 °C) is so sudden that, shortly after reaching the set temperature (**Figure 2**), the residual concentration ($C^{(t)}/C^0$) is close to zero.

The temperature dependence of the anthocyanin degradation rate constant (k) in reconstituted blackberry juice is shown in **Figure 6**. Three regions can be seen: low temperatures (T < 100 °C), where E_a = 37 kJ·mol^{-1} (*7*); intermediate temperatures (100 < T ≤ 140 °C), where E_a = 92 ± 8 kJ·mol^{-1}; and high temperatures (T > 140 °C), where E_a = 44 ± 40 kJ·mol^{-1}.

Although differences in slopes suggest different anthocyanin degradation mechanisms at each temperature range, conclusions cannot be made because studies of reaction mechanisms have been conducted only for low temperatures (T < 100 °C) (*6*). At higher temperatures, many factors may be involved in anthocyanin degradation such as the formation of Maillard reaction products. According to Debicki-Pospisil et al. (*16*) the presence of furfural and 5-(hydroxymethyl) furfural accelerates the degradation rate of cyanidin 3-glucoside in blackberry juice.

Although some kinetic data have been published for high temperatures (*9*, *10*), the optimized parameters shown in **Table 3** present no significant difference with those reported by Harbourne et al. (*9*) for blackcurrant juice at 140 °C (**Table 1**). The relevance of considering heat treatments of more than 100 °C as non-isothermal was confirmed when comparing the kinetic parameters obtained by the traditional 2-step procedure (*9*) for isothermal treatment with those of the non-isothermal method used in our study. For example, in our case, the estimated activation energy (E_a) for $C^{(t)}$ was 92 ± 8 kJ·mol^{-1} (T: [100−140 °C]); whereas, for the same data, if the heat treatments were assumed as isothermal the calculated E_a for $C^{(t)}$ would be 74 kJ·mol^{-1}. The latter value is closer to those reported in literature for heat treatment at T < 100 °C (**Table 1**).

Nonenzymatic Browning. Figure 7 shows the good fit between experimental data and the lower end of the predicted curves, using the kinetic parameters presented in **Table 3** for the nonenzymatic browning index. Good fit is also confirmed by the low root-mean-square error (RMSE = 0.04) and the analysis of residues (**Figure 3c**). The apparent activation energy (E_a) for nonenzymatic browning (T: [100−180 °C]) was slightly higher than the monomeric anthocyanin degradation E_a value at the lower temperature range (92 kJ·mol^{-1}), but was more than twice the value for the higher range (44 kJ·mol^{-1}). However, the reaction rate constant at 140 °C ($k_{140°C}$) for nonenzymatic browning (1.62 × 10^{-3} s^{-1}) was about half the value obtained for anthocyanin degradation (3.5 × 10^{-3} s^{-1}) for T: [100−140 °C].

Therefore, monomeric anthocyanin degradation was faster than the formation of nonenzymatic browning products in reconstituted blackberry juice. This statement shows the importance of improving the understanding of reaction mechanisms involved in anthocyanin degradation and nonenzymatic browning at high temperatures.

Model Applications. Figure 8 illustrates the effect of some simulated high-temperature operations, commonly used in agroindustry, on anthocyanin-rich foodstuffs, assuming similar kinetic parameters (E_a and k_{ref}) as those of our study. From any temperature profile, the behavior of residual anthocyanin concentrations ($C^{(t)}/C^0$) can be predicted throughout the heat treatment.

For example, during deep-fat frying, the temperature range is highly heterogeneous: a dried peripheral region is submitted to high temperature (close to oil temperature), whereas the water-rich core is maintained at temperatures close to 100 °C. As a result, the degradation rate is higher in the food's peripheral regions than at the center (*34*). This may be considered as more of a disadvantage for chips-type products (thin slices) than for French fries-type products (thick slices), which possess a large volume in relation to their surface.

Another example is to compare conventional with high-temperature short-time (HTST) sterilization treatments, using the same *F*-value (here $F_0 = 2.8$ min, with $T_{ref} = 121.11$ °C and $z = 10$ °C), thus demonstrating the advantages of using HTST heat treatments for anthocyanin-rich products to reduce the impact of heat on product quality during different food processes. The equivalent isothermal time β_X, calculated from eq **8** with $T_{ref} = 140$ °C, permits the comparison of anthocyanin degradation across a variety of heat treatments. **Figure 8** shows how the deep-fat frying of thin slices can greatly affect anthocyanin degradation, compared with other operations. Similar effects are also found between spray-drying ($t_{process} = 13$ s) and HTST sterilization ($t_{process} = 150$ s), despite different processing times.

The application of the kinetic model therefore allows the generation and adjustment of temperature profiles of heat processes to better achieve expected results (*35*). Such results may include the improved preservation of the nutritional qualities of heat-sensitive fruits and vegetables during high-temperature processing.

ABBREVIATIONS USED

$C^{(t)}$, monomeric anthocyanins content at time t ($g \cdot L^{-1}$); C^0, monomeric anthocyanins content at time $t = 0$ ($g \cdot L^{-1}$); $B^{(t)}$, nonenzymatic browning index at time t; B^0, nonenzymatic browning index at time $t = 0$; B^∞, nonenzymatic browning index at time $t = \infty$; $X^{(t)} = C^{(t)}$ or $(B^{(t)} - B^\infty)$ at time t; k_X, reaction rate constant of $X^{(t)}$ (s^{-1}); k_{Xiref}, reaction rate constant of $X^{(t)}$ at reference temperature (s^{-1}); E_{aXi}, apparent activation energy of $X^{(t)}$ kinetic ($J \cdot mol^{-1}$); R, gas constant (8.314 $J \cdot mol^{-1} \cdot K^{-1}$); T, temperature (K); T_{ref}, reference temperature (K); t, time (s).

LITERATURE CITED

(1) Siriwoharn, T.; Wrolstad, R. E.; Finn, C. E.; Pereira, C. B. Influence of cultivar, maturity, and sampling on blackberry (*Rubus* L. hybrids) anthocyanins, polyphenolics, and antioxidant properties. *J. Agric. Food Chem.* **2004**, *52*, 8021–8030.

(2) Mertz, C.; Cheynier, V.; Gunata, Z.; Brat, P. Analysis of phenolic compounds in two blackberry species (*Rubus glaucus* and *Rubus adenotrichus*) by high-performance liquid chromatography with diode array detection and electrospray ion trap mass spectrometry. *J. Agric. Food Chem.* **2007**, *55*, 8616–8624.

(3) Prior, R. L., Absorption and Metabolism of Anthocyanins: Potential Health Effects. In *Phytochemicals: Mechanisms of Action*; Meskin, M. S., Bidlack, W. R., Davies, A. J., Lewis, D. S., Randolph, R. K., Eds.; CRC Press: Boca Raton, FL, 2004; pp 1−19.

(4) Clifford, M. N.; Scalbert, A. Ellagitannins—nature, occurrence and dietary burden. *J. Sci. Food Agric.* **2000**, *80*, 1118–1125.

(5) Wrolstad, R. E.; Durst, R. W.; Lee, J. Tracking color and pigment changes in anthocyanin products. *Trends Food Sci. Technol.* **2005**, *16*, 423–428.

(6) Sadilova, E.; Stintzing, F. C.; Carle, R. Thermal degradation of acylated and nonacylated anthocyanins. *J. Food Sci.* **2006**, *71*, C504–C512.

(7) Cisse, M.; Vaillant, F.; Dornier, M.; Acosta, O.; Dhuique-Mayer, C. Thermal degradation kinetics of anthocyanins from blood orange, blackberry and roselle, using the Arrhenius, Eyring and Ball models. *J. Agric. Food Chem.* **2009**, *57*, 6285−6291.

(8) Cao, S. Q.; Liu, L.; Pan, S. Y.; Lu, Q.; Xu, X. Y. A Comparison of Two Determination Methods for Studying Degradation Kinetics of the Major Anthocyanins from Blood Orange. *J. Agric. Food Chem.* **2009**, *57*, 245–249.

(9) Harbourne, N.; Jacquier, J. C.; Morgan, D. J.; Lyng, J. G. Determination of the degradation kinetics of anthocyanins in a model juice system using isothermal and non-isothermal methods. *Food Chem.* **2008**, *111*, 204–208.

(10) Mishra, D. K.; Dolan, K. D.; Yang, L. Confidence intervals for modeling anthocyanin retention in grape pomace during nonisothermal heating. *J. Food Sci.* **2008**, *73*, E9–E15.

(11) Yang, Z. D.; Han, Y. B.; Gu, Z. X.; Fan, G. J.; Chen, Z. G. Thermal degradation kinetics of aqueous anthocyanins and visual color of purple corn (*Zea mays* L.) cob. *Innovative Food Sci. Emerging Technol.* **2008**, *9*, 341–347.

(12) Wang, W. D.; Xu, S. Y. Degradation kinetics of anthocyanins in blackberry juice and concentrate. *J. Food Eng.* **2007**, *82*, 271–275.

(13) Reyes, L. F.; Cisneros-Zevallos, L. Degradation kinetics and colour of anthocyanins in aqueous extracts of purple- and red-flesh potatoes (*Solanum tuberosum* L.). *Food Chem.* **2007**, *100*, 885–894.

(14) Kirca, A.; Ozkan, M.; Cemeroglu, B. Effects of temperature, solid content and pH on the stability of black carrot anthocyanins. *Food Chem.* **2007**, *101*, 212–218.

(15) Cemeroglu, B.; Velioglu, S.; Isik, S. Degradation Kinetics of Anthocyanins in Sour Cherry Juice and Concentrate. *J. Food Sci.* **1994**, *59*, 1216–1218.

(16) Debicki-Pospisil, J.; Lovric, T.; Trinajstic, N.; Sabljic, A. Anthocyanin Degradation in the Presence of Furfural and 5-Hydroxymethylfurfural. *J. Food Sci.* **1983**, *48*, 411–416.

(17) Da Silva, P. F.; Moreira, R. G. Vacuum frying of high-quality fruit and vegetable-based snacks. *LWT—Food Sci. Technol.* **2008**, *41*, 1758–1767.

(18) Camire, M. E.; Chaovanalikit, A.; Dougherty, M. P.; Briggs, J. Blueberry and grape anthocyanins as breakfast cereal colorants. *J. Food Sci.* **2002**, *67*, 438–441.

(19) Tonon, R. V.; Brabet, C.; Hubinger, M. D. Influence of process conditions on the physicochemical properties of acai (*Euterpe oleraceae* Mart.) powder produced by spray drying. *J. Food Eng.* **2008**, *88*, 411–418.

(20) Hessler, J. P. The use of Monte Carlo simulations to evaluate kinetic data and analytic approximations. *Int. J. Chem. Kinet.* **1997**, *29*, 803–817.

(21) AOAC. Fruits and fruits products. In *Official Methods of Analysis of the Association of Official Analytical Chemists International*; Helrich, K., Ed.; Arlington, VA, 1990; pp 910−928.

(22) Giusti, M. M.; Wrolstad, R. E. Anthocyanins. Characterization and Measurement with UV-Visible Spectroscopy. In *Current protocols in food analytical chemistry*; Wrolstad, R. E., Ed.; John Wiley & Sons: New York, 2001, pp F1.2.1−F1.2.13.

(23) Lee, J.; Durst, R. W.; Wrolstad, R. E. Determination of total monomeric anthocyanin pigment content of fruit juices, beverages, natural colorants, and wines by the pH differential method: Collaborative study. *J. AOAC Int.* **2005**, *88*, 1269–1278.

(24) George, S.; Brat, P.; Alter, P.; Amiot, M. J. Rapid determination of polyphenols and vitamin C in plant-derived products. *J. Agric. Food Chem.* **2005**, *53*, 1370–1373.
(25) Ou, B. X.; Hampsch-Woodill, M.; Prior, R. L. Development and validation of an improved oxygen radical absorbance capacity assay using fluorescein as the fluorescent probe. *J. Agric. Food Chem.* **2001**, *49*, 4619–4626.
(26) Gancel, A. L.; Alter, P.; Dhuique-Mayer, C.; Ruales, J.; Vaillant, F. Identifying Carotenoids and Phenolic Compounds In Naranjilla (Solanum quitoense Lam. Var. Puyo Hybrid), an Andean Fruit. *J. Agric. Food Chem.* **2008**, *56*, 11890–11899.
(27) Buglione, M.; Lozano, J. Nonenzymatic browning and chemical changes during grape juice storage. *J. Food Sci.* **2002**, *67*, 1538–1543.
(28) Lagarias, J. C.; Reeds, J. A.; Wright, M. H.; Wright, P. E. Convergence properties of the Nelder-Mead simplex method in low dimensions. *Siam J. Optimiz.* **1998**, *9*, 112–147.
(29) van Boekel, M. A. J. S. Statistical aspects of kinetic modeling for food science problems. *J. Food Sci.* **1996**, *61*, 477–485.
(30) ISO NF ENC 13005. Détermination de l'incertitude élargie. In *Guide pour l'expression de l'incertitude de mesure*; AFNOR: Paris, 1999; pp 39−134.
(31) Benvenuti, S.; Pellati, F.; Melegari, M.; Bertelli, D. Polyphenols, anthocyanins, ascorbic acid, and radical scavenging activity of *Rubus, Ribes,* and *Aronia*. *J. Food Sci.* **2004**, *69*, C164–C169.
(32) Yilmaz, Y.; Toledo, R. Antioxidant activity of water-soluble Maillard reaction products. *Food Chem.* **2005**, *93*, 273–278.
(33) van Boekel, M. A. J. S. *Kinetic modeling of reactions in food*; CRC Press: 2009; pp 7-50−7-60.
(34) Avallone, S.; Rojas-Gonzalez, J. A.; Trystram, G.; Bohuon, P. Thermal Sensitivity of Some Plantain Micronutrients during Deep-Fat Frying. *J. Food Sci.* **2009**, *74*, C339–C347.
(35) Peleg, M.; Normand, M. D.; Corradini, M. G. Interactive software for estimating the efficacy of non-isothermal heat preservation processes. *Int. J. Food Microbiol.* **2008**, *126*, 250–257.

Received for review July 10, 2009. Revised manuscript received December 3, 2009. Accepted December 7, 2009. We are grateful to the EU for funding the PAVUC Project (Contract No. FP6-0015279), and to the French Cultural and Cooperation Centre for Central America (CCCAC, its French acronym) and the University of Costa Rica for their financial support.